Z. Angew. Math. Phys. 62 (2011), 1131–1142

0044-2275/11/061131-12
published online June 23, 2011
DOI 10.1007/s00033-011-0136-1

Zeitschrift für angewandte Mathematik und Physik ZAMP

Stability of anisotropic electroactive polymers with application to layered media

Stephan Rudykh and Gal deBotton

Abstract. The stability of anisotropic electroactive polymers is investigated. A *general* criterion for the onset of instabilities under plane-strain conditions is introduced in terms of a sextic polynomial whose coefficients depend on the instantaneous electroelastic moduli. In a way of an example, the stable domains of layered neo-Hookean dielectrics are determined. It is found that depending on the direction of the electrostatic excitation field relative to the lamination direction, the critical stretch ratios at which instabilities may occur can be either larger or smaller than the ones for the purely mechanical case.

Mathematics Subject Classification (2000). 74B20 · 74G60 · 74F15 · 78A30 · 37C20.

Keywords. Electroactive polymers · Dielectric elastomers · Finite deformations · Anisotropy · Non-linear electroelasticity.

1. Introduction

Electroactive polymers (EAP) are promising materials which enable to convert electrical energy into mechanical one [5,19,20]. The basic theory of the elastic dielectric was developed by Toupin [28] and was recently revisited by McMeeking and Landis [16], Dorfmann and Ogden [10] and Vu and Steinmann [31]. The class of transversely isotropic materials was considered by Bustamante [6]. Wide-spread usage of EAPs is limited because of the need for large electric fields [2,24]. To overcome this difficulty the usage of heterogeneous electroactive materials was proposed recently by Zhang et al. [14,32]. Indeed, recent theoretical works demonstrate that this approach may lead to marked enhancement of the electromechanical coupling (*e.g.,* deBotton et al. [9] and Tian et al. [27]). Clearly, a comprehensive investigation of these composite dielectrics is significant toward overcoming their limitations and advancing their implementation in "real life" applications. In this regard, an important aspect of the behavior of EAP composites concerns the possible developments of instabilities under certain electromechanical loading conditions.

Commonly, the instability phenomenon is considered as a negative one that should be predicted and avoided. However, in some cases, it can be used for our benefit. For example, as a trigger for large deformations [17,23] or as a wave guide filtering [12]. Electromechanical instabilities in homogeneous electroactive materials such as pull-in instabilities [21] and electrical breakdown [15] were studied experimentally. Theoretical study of the incremental governing equations was conducted by Dorfmann and Ogden [11]. More recently, Bertoldi and Gei [4] investigated instabilities in soft neo-Hookean layered dielectrics in which the electric field is perpendicular to the layers and pre-stretch is applied along the layers.

In this study, we examine the stable domain of *anisotropic* electroactive materials undergoing large deformations. We introduce a *general condition* for the onset of instability in plane problem. In a way of an example, we examine the class of layered media with isotropic behavior of the layers. We chose this class for two reasons. The first is related to the fact that expressions for the coupled electromechanical behaviors of anisotropic EAPs are not available in the literature, and since layered materials can be manufactured, the outcome will correspond to a feasible class of anisotropic materials. For this reason, we also chose a widely accepted form for the phases behavior, one that can provides an approximation to more complicated behaviors in the limit of small to moderate deformations. The second reason stems

from the fact that for this class of materials a rigorous *explicit* expression for the homogenized anisotropic energy-density function can be determined [4,8]. By making use of this expression for their overall energy-density function, we identify the stable domain of these materials under different loading conditions and demonstrate the significance of their overall symmetry.

In passing, we recall that in heterogeneous materials instabilities at different wavelengths may appear [30]. These may range from the size of a typical inhomogeneity to that of many representative volume elements. In the purely mechanical case it was shown by Geymonat et al. [13] that stability analyses of the homogenized constitutive behavior correspond to the long wave limit. This implies that along different loading paths instabilities at shorter wavelengths may precede the macroscopic ones. Thus, the stable domain that is determined by analyzing the homogenized constitutive behavior of a composite provides an upper bound for its actual stable domain. In this study, we do not consider instabilities other than the macroscopic ones as our goal is to analyze the significance of *anisotropy* on the stable domain of electroactive materials. To this end, we exploit the fact that an explicit expression for the overall behavior of layered dielectrics can be determined and make use of this expression as a representative one for the class of anisotropic materials.

The work is structured as follows: in the next section we start with the required theoretical background and continue with the introduction of the criterion for the onset of instability in anisotropic EAPs under plane-strain conditions. This is followed by a derivation of the effective energy-density function for layered composites and a few numerical examples that highlight the dependency of the bifurcation diagrams on anisotropy along different loading paths.

2. Theory

The Cartesian position vector of a material point in a reference configuration of a body $\mathscr{B}_0$ is $\mathbf{X}$, and its position vector in the deformed configuration $\mathscr{B}$ is $\mathbf{x}$. The deformation of the body is characterized by the mapping $\mathbf{x}=\boldsymbol{\chi}(\mathbf{X})$. The deformation gradient is $\mathbf{F}=\dfrac{\partial\boldsymbol{\chi}(\mathbf{X})}{\partial\mathbf{X}}$. We assume that the deformation is invertible and hence $\mathbf{F}$ is non-singular. Accordingly, $J\equiv\det\mathbf{F}\neq 0$. Furthermore, since J is the volume ratio between the volumes of an element in the deformed and the reference configurations, on physical ground, we assume that $J=\dfrac{\mathrm{d}v}{\mathrm{d}V}>0$.

The differential operators in the reference configuration are denoted Div$(\bullet)$ and Curl$(\bullet)$, and the corresponding operators in the current configuration are div$(\bullet)$ and curl$(\bullet)$, respectively. We assume that the deformation is quasi-static and no magnetic field is present. Consequently, Maxwell equations reduce to

$$\mathrm{div}\mathbf{D}=0,\quad \mathrm{curl}\mathbf{E}=0. \tag{1}$$

Here, $\mathbf{D}$ is the electric displacement, and $\mathbf{E}$ is the electric field in the *current* configuration.

Following Dorfmann and Ogden [10], these equations can be rewritten in terms of the referential electric field $\mathbf{E}^0=\mathbf{F}^T\mathbf{E}$ and the referential electric displacement $\mathbf{D}^0=J\mathbf{F}^{-1}\mathbf{D}$ as

$$\mathrm{Div}\mathbf{D}^0=0\quad\text{and}\quad\mathrm{Curl}\mathbf{E}^0=0. \tag{2}$$

In the absence of body forces, the equilibrium equation is

$$\mathrm{Div}\mathbf{P}=0, \tag{3}$$

where $\mathbf{P}$ is the *total* nominal stress tensor. The corresponding total true or Cauchy stress tensor is related to the nominal stress tensor via the relation $\sigma=J^{-1}\mathbf{P}\mathbf{F}^T$. We consider hyperelastic dielectrics whose behaviors are characterized by a scalar-valued *augmented* energy-density function $\Psi(\mathbf{F},\mathbf{D}^0)$ such that

$$\mathbf{P}=\frac{\partial\Psi(\mathbf{F},\mathbf{D}^0)}{\partial\mathbf{F}}\quad\text{and}\quad\mathbf{E}^0=\frac{\partial\Psi(\mathbf{F},\mathbf{D}^0)}{\partial\mathbf{D}^0}. \tag{4}$$

For the class of incompressible materials

$$\mathbf{P} = \frac{\partial \Psi(\mathbf{F}, \mathbf{D}^0)}{\partial \mathbf{F}} + p\mathbf{F}^{-T}, \tag{5}$$

where p is a pressure-like Lagrange multiplier, and the expression for $\mathbf{E}^0$ is similar to the one in Eq. (4).

The incremental governing equations are (Dorfmann and Ogden [11])

$$\mathrm{Div}\dot{\mathbf{P}} = 0, \quad \mathrm{Div}\dot{\mathbf{D}}^0 = 0 \quad \text{and} \quad \mathrm{Curl}\dot{\mathbf{E}}^0 = 0, \tag{6}$$

where $\dot{\mathbf{P}}, \dot{\mathbf{D}}^0$, and $\dot{\mathbf{E}}^0$ are infinitesimal increments in the nominal stress, the referential electric displacement and the referential electrical field, respectively. The linearized constitutive equations are expressed in terms of the electroelastic moduli tensors

$$\mathscr{A}^0_{\alpha j \beta l} = \frac{\partial^2 \Psi}{\partial F_{\alpha j} \partial F_{\beta l}}, \quad \mathscr{G}^0_{i\alpha\beta} = \frac{\partial^2 \Psi}{\partial F_{i\alpha} \partial D^0_\beta}, \quad \mathscr{E}^0_{\alpha\beta} = \frac{\partial^2 \Psi}{\partial D^0_\alpha \partial D^0_\beta}, \tag{7}$$

such that

$$\dot{P}_{ij} = \mathscr{A}^0_{ijkl}\dot{F}_{kl} + \mathscr{G}^0_{ijk}\dot{D}^0_k \quad \text{and} \quad \dot{E}_i = \mathscr{G}^0_{jki}\dot{F}_{jk} + \mathscr{E}^0_{ij}\dot{D}^0_j. \tag{8}$$

For an incompressible material, the linearized constitutive relations are

$$\dot{P}_{ij} = \mathscr{A}^0_{ijkl}\dot{F}_{kl} + \mathscr{G}^0_{ijk}\dot{D}^0_k - \dot{p}F^{-T}_{ij} + pF^{-1}_{jk}\dot{F}_{kl}F^{-1}_{li} \tag{9}$$

and

$$\dot{E}_i = \mathscr{G}^0_{jki}\dot{F}_{jk} + \mathscr{E}^0_{ij}\dot{D}^0_j, \tag{10}$$

where $\dot{p}$ is an incremental change in p.

Consider, next, the current configuration as a new reference configuration. We recall that $\dot{F}_{kl} = v_{k,n}F_{nl}$, where $v_i = \dot{x}_i$ is an increment in x_i. The corresponding counterparts of $\dot{\mathbf{P}}, \dot{\mathbf{E}}^0$, and $\dot{\mathbf{D}}^0$ in the current configuration are

$$\hat{\mathbf{T}} = J^{-1}\dot{\mathbf{P}}\mathbf{F}^T, \quad \hat{\mathbf{D}} = J^{-1}\mathbf{F}\dot{\mathbf{D}}^0 \quad \text{and} \quad \hat{\mathbf{E}} = \mathbf{F}^{-T}\dot{\mathbf{E}}^0. \tag{11}$$

Following Dorfmann and Ogden [11] once again, the corresponding incremental governing Eq. (6) are

$$\mathrm{div}\hat{\mathbf{T}} = 0, \quad \mathrm{div}\hat{\mathbf{D}} = 0, \quad \mathrm{curl}\hat{\mathbf{E}} = 0. \tag{12}$$

In this configuration, the linearized constitutive equations are

$$\hat{T}_{ij} = \mathscr{A}_{ijkl}v_{k,l} + \mathscr{G}_{ijk}\hat{D}_k - \dot{p}\delta_{ij} + pv_{j,i} \tag{13}$$

and

$$\hat{E}_i = \mathscr{G}_{jki}v_{j,k} + \mathscr{E}_{ij}\hat{D}_j, \tag{14}$$

where

$$\mathscr{A}_{ijkl} = J^{-1}F_{j\alpha}F_{l\beta}\mathscr{A}^0_{i\alpha k\beta}, \quad \mathscr{G}_{ijk} = F_{j\alpha}F^{-1}_{\beta k}\mathscr{G}^0_{i\alpha\beta} \quad \text{and} \quad \mathscr{E}_{ij} = JF^{-1}_{\alpha i}F^{-1}_{\beta j}\mathscr{E}^0_{\alpha\beta}. \tag{15}$$

These electroelastic moduli tensors possess the symmetries

$$\mathscr{A}_{ijkl} = \mathscr{A}_{klij}, \quad \mathscr{G}_{ijk} = \mathscr{G}_{jik} \quad \text{and} \quad \mathscr{E}_{ij} = \mathscr{E}_{ji}. \tag{16}$$

Upon substitution of the linearized constitutive relations (13) and (14) in the governing Eq. (12), the following equations are revealed

$$\mathscr{A}_{ijkl}v_{k,lj} + \mathscr{G}_{ijk}\hat{D}_{k,j} - \dot{p}_{,i} = 0, \quad e_{spi}\left(\mathscr{G}_{jki}v_{j,kp} + \mathscr{E}_{ij}\hat{D}_{j,p}\right) = 0, \tag{17}$$

where e_{spi} is the Levi-Civita symbol.

In order to determine the onset of instabilities, we seek a solution for Eq. (17) in the form

$$v_i = \tilde{v}_i f(\hat{\mathbf{a}} \cdot \mathbf{x}), \quad \dot{p} = \tilde{q} f'(\hat{\mathbf{a}} \cdot \mathbf{x}), \quad \hat{D}_i = \tilde{d}_i f'(\hat{\mathbf{a}} \cdot \mathbf{x}), \tag{18}$$

where f is a continuous and sufficiently differentiable function, and $\hat{\mathbf{a}}$ is a unit vector.

We assume that the material undergoes *plane-strain* deformations and there is no out-of-plane component of the electric displacement field. In this case, by making use of the incompressibility constraint $\operatorname{div}\mathbf{v}=0$ together with Maxwell equation for $\hat{\mathbf{D}}$, we find that $\tilde{v}_i\hat{a}_i=0$ and $\tilde{d}_i\hat{a}_i=0$ and hence $\tilde{d}_i=\gamma\tilde{v}_i$, where γ is a real coefficient. Thus, upon substitution of Eq. (18) together with the relation $\tilde{d}_i=\gamma\tilde{v}_i$ in Eq. (17) and eliminating the pressure increment, we end up with a polynomial equation for $\xi\equiv a_2/a_1$, namely

$$\Gamma_6\xi^6+\Gamma_5\xi^5+\Gamma_4\xi^4+\Gamma_3\xi^3+\Gamma_2\xi^2+\Gamma_1\xi+\Gamma_0=0. \tag{19}$$

The coefficients Γ_i are given in terms of the electroelastic moduli

$$\begin{aligned}
\Gamma_0&=\mathscr{G}_{122}^2-\mathscr{A}_{2121}\mathscr{E}_{22},\\
\Gamma_1&=2\left(\mathscr{A}_{2121}\mathscr{E}_{12}+\left(\mathscr{A}_{1121}-\mathscr{A}_{2122}\right)\mathscr{E}_{22}-\mathscr{G}_{122}\left(\mathscr{G}_{112}+\mathscr{G}_{121}-\mathscr{G}_{222}\right)\right),\\
\Gamma_2&=-\mathscr{A}_{2121}\mathscr{E}_{11}-4\left(\mathscr{A}_{1121}-\mathscr{A}_{2122}\right)\mathscr{E}_{12}-\left(\mathscr{A}_{1111}-2\mathscr{A}_{1122}-2\mathscr{A}_{1221}+\mathscr{A}_{2222}\right)\mathscr{E}_{22}\\
&\quad+2\mathscr{G}_{122}\left(\mathscr{G}_{111}-\mathscr{G}_{122}-\mathscr{G}_{221}\right)+\left(\mathscr{G}_{112}+\mathscr{G}_{121}-\mathscr{G}_{222}\right)^2,\\
\Gamma_3&=2\left(\left(\mathscr{A}_{1121}-\mathscr{A}_{2122}\right)\mathscr{E}_{11}+\left(\mathscr{A}_{1111}-2\mathscr{A}_{1122}-2\mathscr{A}_{1221}+\mathscr{A}_{2222}\right)\mathscr{E}_{12}\right.\\
&\quad\left.+\left(\mathscr{A}_{1222}-\mathscr{A}_{1112}\right)\mathscr{E}_{22}+\left(\mathscr{G}_{121}\mathscr{G}_{122}-\left(\mathscr{G}_{111}-\mathscr{G}_{122}-\mathscr{G}_{221}\right)\left(\mathscr{G}_{112}+\mathscr{G}_{121}-\mathscr{G}_{222}\right)\right)\right),\\
\Gamma_4&=-\left(\mathscr{A}_{1111}-2\mathscr{A}_{1122}-2\mathscr{A}_{1221}+\mathscr{A}_{2222}\right)\mathscr{E}_{11}+4\left(\mathscr{A}_{1112}-\mathscr{A}_{1222}\right)\mathscr{E}_{12}\\
&\quad-\mathscr{A}_{1212}\mathscr{E}_{22}+\left(\mathscr{G}_{122}+\mathscr{G}_{221}-\mathscr{G}_{111}\right)^2-2\mathscr{G}_{121}\left(\mathscr{G}_{112}+\mathscr{G}_{121}-\mathscr{G}_{222}\right),\\
\Gamma_5&=2\left(\left(\mathscr{A}_{1222}-\mathscr{A}_{1112}\right)\mathscr{E}_{11}+\mathscr{A}_{1212}\mathscr{E}_{12}+\mathscr{G}_{121}\left(\mathscr{G}_{111}-\mathscr{G}_{122}-\mathscr{G}_{221}\right)\right),\\
\Gamma_6&=\mathscr{G}_{121}^2-\mathscr{A}_{1212}\mathscr{E}_{11}.
\end{aligned} \tag{20}$$

Whenever a real solution for Eq. (19) exists, instabilities may occur. The corresponding value of γ that relates the amplitudes of the incremental changes in the electric displacement and the displacement is

$$\gamma=\frac{\mathscr{G}_{121}\xi^3+\left(\mathscr{G}_{111}-\mathscr{G}_{122}-\mathscr{G}_{221}\right)\xi^2+\left(\mathscr{G}_{222}-\mathscr{G}_{112}-\mathscr{G}_{121}\right)\xi+\mathscr{G}_{122}}{\mathscr{E}_{22}+\left(\mathscr{E}_{11}\xi-2\mathscr{E}_{12}\right)\xi}. \tag{21}$$

We conclude this section noting that condition (19) is an extension to the class of anisotropic materials of the corresponding result derived by Dorfmann and Ogden [11] for the class of isotropic materials. In the following section, we apply this general criterion to a specific class of anisotropic materials for which analytical expressions for the electroelastic moduli can be determined. Yet, before we proceed to this task, we stress that condition (19) can be used in conjunction with numerical simulations of more general anisotropic materials for which analytical solutions cannot be determined. In these cases estimates for the electroelastic moduli can be determined with appropriate simulations of small variations in the boundary conditions.

3. Applications to soft dielectric laminates

In a way of an example, we examine the class of layered composites with two isotropic and incompressible phases. As was mentioned in the introduction, from a practical viewpoint, this is a feasible class of materials and, from a theoretical viewpoint, their overall behavior can be determined explicitly (deBotton et al. [9]; Tevet-Deree [26]). The resulting closed form expressions for the electroelastic moduli can be conveniently utilized in the stability analysis. Bertoldi and Gei [4] considered this class of composites under specific loading conditions that are aligned with the layers. Here, we extend this analysis and examine the influence of more general loadings on the onset of instabilities. In this regard, it is worth mentioning that enhancement of the mechanical response to electrical excitation crucially depends on the ability to furnish appropriate soft modes of deformation by controlling the angle between the layers and the electrical excitation field [9,26].

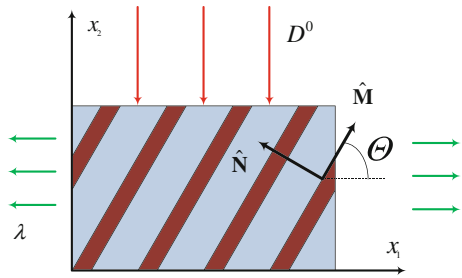

FIG. 1. Electroactive layered composite subjected to electric excitation

The volume fractions of the phases are $c^{(m)}$ and $c^{(f)} = 1 - c^{(m)}$. Geometrically, the layers are characterized by their thicknesses $h^{(m)} = c^{(m)}h$ and $h^{(f)} = c^{(f)}h$, where $h = h^{(m)} + h^{(f)}$. Here and thereafter, we denote a field in phase r by $(\bullet)^{(r)}$, in particular $(\bullet)^{(f)}$ and $(\bullet)^{(m)}$ correspond to the stiffer and the softer phases, respectively. The direction normal to the layers plane in the undeformed configuration is the laminate direction $\hat{\mathbf{N}}$, and $\hat{\mathbf{M}}$ is a unit vector tangent to the interface (see Fig. 1). Specifically, in terms of the referential lamination angle Θ,

$$\hat{\mathbf{N}} = \sin\Theta\,\hat{\mathbf{e}}_1 + \cos\Theta\,\hat{\mathbf{e}}_2 \quad \text{and} \quad \hat{\mathbf{M}} = \cos\Theta\,\hat{\mathbf{e}}_1 - \sin\Theta\,\hat{\mathbf{e}}_2. \tag{22}$$

Assuming that all fields are homogeneous in each phase, we have that the mean deformation gradient, the nominal electric field and the electric displacement are

$$\bar{\mathbf{F}} = c^{(m)}\mathbf{F}^{(m)} + c^{(f)}\mathbf{F}^{(f)}, \quad \bar{\mathbf{E}}^0 = c^{(m)}\mathbf{E}^{0\,(m)} + c^{(f)}\mathbf{E}^{0\,(f)}, \quad \bar{\mathbf{D}}^0 = c^{(m)}\mathbf{D}^{0\,(m)} + c^{(f)}\mathbf{D}^{0\,(f)}. \tag{23}$$

Following deBotton [7], by making use of the displacement continuity condition across the interface

$$\mathbf{F}^{(m)} = \bar{\mathbf{F}}\left(\mathbf{I} + c^{(f)}\alpha\hat{\mathbf{M}}\otimes\hat{\mathbf{N}}\right), \quad \mathbf{F}^{(f)} = \bar{\mathbf{F}}\left(\mathbf{I} - c^{(m)}\alpha\hat{\mathbf{M}}\otimes\hat{\mathbf{N}}\right), \tag{24}$$

where the scalar α is obtained from the traction continuity condition

$$\left(\mathbf{P}^{(m)} - \mathbf{P}^{(f)}\right)\cdot\hat{\mathbf{N}} = 0. \tag{25}$$

Similarly, since the interfaces are charge free, the continuity condition for the electric displacement is

$$\left(\mathbf{D}^{0\,(m)} - \mathbf{D}^{0\,(f)}\right)\cdot\hat{\mathbf{N}} = 0 \quad \text{or} \quad \mathbf{D}^{0\,(m)} - \mathbf{D}^{0\,(f)} = \beta\hat{\mathbf{M}}, \tag{26}$$

and, together with the last of Eq. (23), we conclude that

$$\mathbf{D}^{0\,(m)} = \bar{\mathbf{D}}^0 + c^{(f)}\beta\hat{\mathbf{M}} \quad \text{and} \quad \mathbf{D}^{0\,(f)} = \bar{\mathbf{D}}^0 - c^{(m)}\beta\hat{\mathbf{M}}, \tag{27}$$

where β is a scalar to be determined from the continuity condition for the nominal electric field

$$\left(\mathbf{E}^{0\,(m)} - \mathbf{E}^{0\,(f)}\right)\cdot\hat{\mathbf{M}} = 0. \tag{28}$$

The energy-density functions of the isotropic phases can be expressed in terms of the invariants of the Cauchy–Green strain tensor $\mathbf{C} \equiv \mathbf{F}^T\mathbf{F}$ and the referential electric displacement $\mathbf{D}^0$ [10]. A set of six invariants can be expressed in the form

$$\begin{aligned} &I_1 = \mathrm{Tr}\mathbf{C}, \quad I_2 = \frac{1}{2}\left(I_1^2 - \mathrm{Tr}(\mathbf{C}\mathbf{C})\right), \quad I_3 = \det\mathbf{C}, \\ &I_{4e} = \mathbf{D}^0\cdot\mathbf{D}^0, \quad I_{5e} = \mathbf{D}^0\cdot\mathbf{C}\mathbf{D}^0, \quad I_{6e} = \mathbf{D}^0\cdot\mathbf{C}^2\mathbf{D}^0. \end{aligned} \tag{29}$$

Thus, the energy-density functions of the isotropic phases can be written as scalar functions of these six invariants in terms of the local fields $\mathbf{F}^{(r)}$ and $\mathbf{D}^{0\,(r)}$. In particular, for composites with neo-Hookean dielectric phases the energy-density functions are

$$\Psi^{(r)}(\mathbf{F}^{(r)},\mathbf{D}^{0\,(r)})=\frac{\mu^{(r)}}{2}\left(I_1^{(r)}-3\right)+\frac{1}{2\varepsilon^{(r)}}I_{5e}^{(r)}, \tag{30}$$

where $\mu^{(r)}$ are the shear moduli, and $\varepsilon^{(r)}$ are the dielectric constants of the two phases. In this work, we restrict our attention to this class of phases behaviors for two reasons. The first stems from the fact that explicit expressions for the corresponding effective electroelastic moduli can be determined. The second is that, at moderate stretch levels where instabilities frequently onset, this energy-density function can be viewed as a first-order estimate for more general energy-density functions [*e.g.,* 25]. Moreover, in the purely mechanical case, it was recently found that the critical stretch ratios at which instabilities occur in composites with neo-Hookean phases can serve as good estimates for corresponding critical stretch ratios for composites with Gent phases [1,3,22].

Upon substitution of Eq. (30), with the aid of Eq. (5) for $\mathbf{P}^{(r)}$ and $\mathbf{E}^{0(r)}$, in Eqs. (25) and (28), we find that

$$\alpha=\frac{\mu^{(f)}-\mu^{(m)}}{c^{(m)}\mu^{(f)}+c^{(f)}\mu^{(m)}}\frac{\bar{\mathbf{F}}\hat{\mathbf{N}}\cdot\bar{\mathbf{F}}\hat{\mathbf{M}}}{\bar{\mathbf{F}}\hat{\mathbf{M}}\cdot\bar{\mathbf{F}}\hat{\mathbf{M}}}, \tag{31}$$

where

$$\beta=\frac{\mu^{(m)}\varepsilon^{(m)}-\mu^{(f)}\varepsilon^{(f)}}{\left(c^{(m)}\mu^{(f)}+c^{(f)}\mu^{(m)}\right)\bar{\varepsilon}}\frac{\bar{\mathbf{F}}\bar{\mathbf{D}}^0\cdot\bar{\mathbf{F}}\hat{\mathbf{M}}}{\bar{\mathbf{F}}\hat{\mathbf{M}}\cdot\bar{\mathbf{F}}\hat{\mathbf{M}}}+\frac{\mu^{(f)}-\mu^{(m)}}{c^{(m)}\mu^{(f)}+c^{(f)}\mu^{(m)}}\bar{\mathbf{D}}^0\cdot\hat{\mathbf{M}}, \tag{32}$$

and $\bar{\varepsilon}=c^{(m)}\varepsilon^{(m)}+c^{(f)}\varepsilon^{(f)}$.

Once the solution for the boundary value problem is given in terms of the local fields in both phases, the expression for the macroscopic energy-density function of the composite can be expressed as the weighted sum of the energy-density functions of the two phases, namely

$$\tilde{\Psi}(\bar{\mathbf{F}},\bar{\mathbf{D}}^0)=\sum_{r=m,f}c^{(r)}\Psi^{(r)}(\bar{\mathbf{F}},\bar{\mathbf{D}}^0). \tag{33}$$

The expressions for the average nominal stress and electric field are

$$\bar{\mathbf{P}}=\frac{1}{2}\sum_{r=m,f}c^{(r)}\left(\mu^{(r)}\frac{\partial I_1^{(r)}}{\partial\bar{\mathbf{F}}}+\frac{1}{\varepsilon^{(r)}}\frac{\partial I_5^{(r)}}{\partial\bar{\mathbf{F}}}\right)-p\bar{\mathbf{F}}^{-T}, \tag{34}$$

and

$$\bar{\mathbf{E}}^0=\frac{1}{2}\sum_{r=m,f}\frac{c^{(r)}}{\varepsilon^{(r)}}\frac{\partial I_5^{(r)}}{\partial\bar{\mathbf{D}}^0}. \tag{35}$$

The corresponding overall electroelastic moduli are

$$\begin{aligned}\mathscr{A}^0_{ijkl}&=\frac{1}{2}\sum_{r=m,f}c^{(r)}\left(\mu^{(r)}\frac{\partial^2 I_1^{(r)}}{\partial\bar{\mathbf{F}}\partial\bar{\mathbf{F}}}+\frac{1}{\varepsilon^{(r)}}\frac{\partial^2 I_5^{(r)}}{\partial\bar{\mathbf{F}}\partial\bar{\mathbf{F}}}\right),\\ \mathscr{G}^0_{ijk}&=\frac{1}{2}\sum_{r=m,f}\frac{c^{(r)}}{\varepsilon^{(r)}}\frac{\partial^2 I_5^{(r)}}{\partial\bar{\mathbf{F}}\partial\bar{\mathbf{D}}^0},\\ \mathscr{E}^0_{ij}&=\frac{1}{2}\sum_{r=m,f}\frac{c^{(r)}}{\varepsilon^{(r)}}\frac{\partial^2 I_5^{(r)}}{\partial\bar{\mathbf{D}}^0\partial\bar{\mathbf{D}}^0}.\end{aligned} \tag{36}$$

Finally, with the aid of Eq. (20), the appropriate coefficients can be determined and substituted in the general instability condition (19).

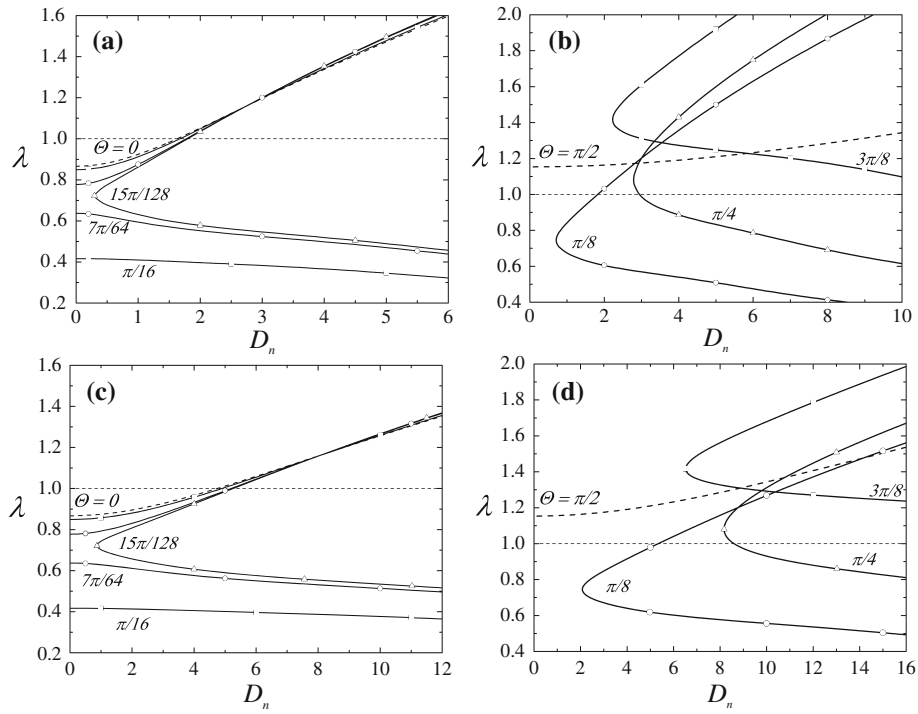

FIG. 2. Bifurcation diagrams of layered materials with different lamination angles as functions of the critical stretch ratio and electric displacement field. The volume fractions of the stiffer phase is $c^{(f)} = 0.2$ for (**a**) and (**b**) and $c^{(f)} = 0.8$ for (**c**) and (**d**); the phase constants ratios are $k = t = 10$. Figures (**a**) and (**c**) are for small lamination angles, and figures (**b**) and (**d**) are for large lamination angles

We examine the behavior of a composite which is subjected to electric excitation corresponding to a nominal electric displacement in the form

$$\bar{\mathbf{D}}^0 = \bar{D}^0 (\cos\varphi \hat{\mathbf{e}}_1 + \sin\varphi \hat{\mathbf{e}}_2), \tag{37}$$

and macroscopically stretched according to the homogeneous deformation gradient

$$\bar{\mathbf{F}} = \lambda \hat{\mathbf{e}}_1 \otimes \hat{\mathbf{e}}_1 + \lambda^{-1} \hat{\mathbf{e}}_2 \otimes \hat{\mathbf{e}}_2 + \hat{\mathbf{e}}_3 \otimes \hat{\mathbf{e}}_3. \tag{38}$$

We consider first the case $\varphi = \pi/2$ and the angle of lamination relative to the applied loading varies. The loading configuration is schematically shown in Fig. 1. We make use of Eqs. (19) and (36) to determine the stable domain of the layered EAP.

Shown in Fig. 2 are the analytical estimates for the onset of instabilities in materials with $c^{(f)} = 0.2$ (Fig. 2a, b) and $c^{(f)} = 0.8$ (Fig. 2c, d), stiffer-to-softer shear moduli ratio $k \equiv \mu^{(f)}/\mu^{(m)} = 10$ and dielectric constants ratio $t \equiv \varepsilon^{(f)}/\varepsilon^{(m)} = 10$. Following Triantafyllidis et al. [30], we plot *failure surfaces* that separate stable domains from these in which instabilities may develop. These bifurcation diagrams are presented as functions of the critical stretch ratio λ_c and the critical electrostatic excitation $D_n = \bar{D}^0/\sqrt{\mu^{(m)}\varepsilon^{(m)}}$ for composites with different lamination angles. The dashed curves for $\Theta = 0$ in Fig. 2a, c are identical to the ones determined by Bertoldi and Gei [4].

We note that in agreement with earlier findings [*e.g.,* 1,18,22,29], in the purely mechanical case ($D_n = 0$), the composites become unstable only under compression in the layers direction. Moreover, as the angle between the loading and the lamination directions increases, there exists an angle beyond which no macroscopic instability occurs [1]. This corresponds to the situation where the layers rotate to

an angle $\theta = \pi/4$ in the deformed configuration [22]. At this angle the loading on the layers switches from compression to tension. Consequently, beyond this point no instability is detected. In contrast to the purely mechanical case, under coupled electromechanical loadings instabilities may develop in composites with lamination angles beyond the critical one. The failure surfaces of composites with lamination angles smaller than the critical angle are shown in Fig. 2a, c, and these of composites with lamination angles larger than the critical one are shown in Fig. 2b, d. To highlight the transition from small to large lamination angles we added the curves for the failure surface of a composite with lamination angle slightly larger than the critical angle ($\Theta = 15\pi/128$) to Fig. 2a, c.

We observe that, in a manner similar to one observed in the purely mechanical case, at low electrostatic fields an increase in the lamination angle stabilizes the composites. However, this effect decays as the applied excitation field is increased and beyond a certain value the effect is reversed. Specifically, as can be seen in Fig. 2a, c, at values of D_n larger than ~ 3.0 for $c^{(f)} = 0.2$ and ~ 10.0 for $c^{(f)} = 0.8$, an increase in Θ may result in earlier onsets of instabilities.

We note that whenever $\Theta = n\pi$ and $\pi/2 + n\pi$, or $n = 0, 1, 2\ldots$, the coefficients $\Gamma_1, \Gamma_3, \Gamma_5$ in Eq. (19) vanish and the condition for ellipticity loss can be written in terms of the bi-cubic polynomial

$$\Gamma_6\xi^6 + \Gamma_4\xi^4 + \Gamma_2\xi^2 + \Gamma_0 = 0. \tag{39}$$

For the case $\Theta = 0$, this result was previously determined by Bertoldi and Gei [4]. The corresponding relation between the critical stretch ratio and the electric excitation is

$$\lambda_c = \left(1 - \frac{\check{\mu}}{\bar{\mu}} + \frac{D^2}{\bar{\mu}\check{\varepsilon}}\left(1 - \frac{\check{\varepsilon}}{\bar{\varepsilon}}\right)\right)^{1/4}, \tag{40}$$

where $\check{\varepsilon} = \left(c^{(m)}/\varepsilon^{(m)} + c^{(f)}/\varepsilon^{(f)}\right)^{-1}$, $\check{\mu} = \left(c^{(m)}/\mu^{(m)} + c^{(f)}/\mu^{(f)}\right)^{-1}$, and $\bar{\mu} = c^{(m)}\mu^{(m)} + c^{(f)}\mu^{(f)}$. Here, we find that for the case $\Theta = \pi/2$, the critical stretch ratio is

$$\lambda_c = \left(1 - \frac{\check{\mu}}{\bar{\mu}}\right)^{-1/4}\left(1 - \frac{D^2}{\bar{\mu}\check{\varepsilon}}\left(1 - \frac{\check{\varepsilon}}{\bar{\varepsilon}}\right)\right)^{1/4}. \tag{41}$$

In the purely mechanical case ($D_n = 0$), both expressions (40) and (41) appropriately reduce to the well-known result of Triantafyllidis and Maker [29].

The bifurcation diagrams of composites with phase volume fractions $c^{(f)} = 0.2$ and material constants similar to the ones considered previously are shown in Fig. 3. To highlight the role of the anisotropy of the material this time the critical stretch ratios are presented as functions of the lamination angle for different electrostatic loading conditions. The curves with square, triangle, white circle, and black circle marks correspond to excitation fields $D_n = 1.37, 2.05, 2.73$, and 4.0, respectively. The dashed curve represents the purely mechanical case. This curve is symmetric with respect to the loading direction $\Theta = 0$, that is $\lambda_c(\Theta) = \lambda_c(-\Theta)$, and is also π-periodic, that is, $\lambda_c(\Theta) = \lambda_c(\Theta + \pi j)$, $\quad j = 1, 2, 3\ldots$. Additionally, we note that $\lambda_c(\Theta) = 1/\lambda_c(\Theta + \pi/2)$. In contrast to the purely mechanical case, in general, the electromechanical failure surfaces do not possess the last symmetry due to the different contributions of the electric excitation in the two perpendicular cases.

We observe that in the purely mechanical case composites with larger lamination angles are becoming more stable [18]. This is also true at moderate levels of electric excitations where we note that the topmost curves that emerge from the $\Theta = 0$ axis have a negative slope up to a certain lamination angle beyond which no instability is detected. However, at large enough electrostatic excitation, the direction of the slope is reversed (*e.g.,* the curve marked by black circles that corresponds to $\bar{\mathbf{D}}_n = 4.0$). Furthermore, under large electrostatic fields, instabilities may occur at any lamination angle.

A somewhat different observation is associated with the case where the layers are aligned with the electric field (*i.e.,* $\Theta = \pi/2$). In this limit the electric field stabilizes the material and larger tensile stretch ratios (that correspond to larger compressions along the layers) are required for the onset of instabilities. At moderate levels of electric fields, as the lamination angle of the composite is decreased toward $\Theta = 0$,

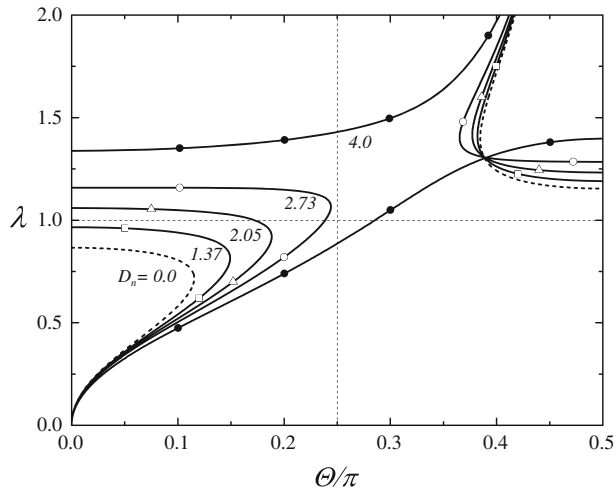

FIG. 3. Bifurcation diagrams of layered materials as functions of the critical stretch ratio and the lamination angle at different levels of electric excitations. The volume fraction of the stiffer phase is $c^{(f)} = 0.2$, the shear moduli ratio is $k = 10$, and the dielectric constants ratio is $t = 10$

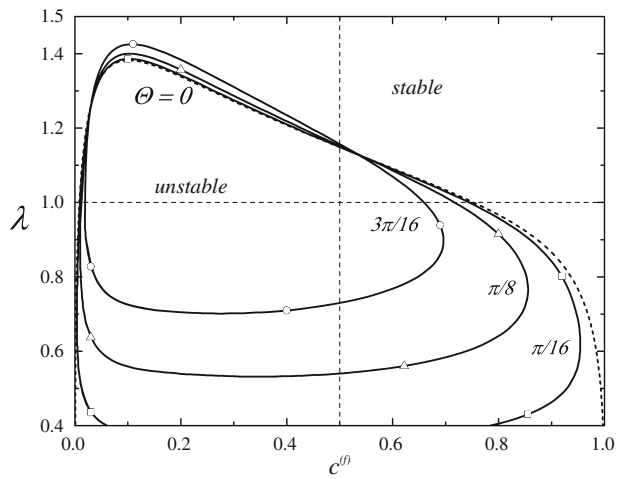

FIG. 4. The failure surfaces of layered composites with different lamination angles as functions of the critical stretch ratio and volume fraction of the stiffer phase subjected to a fixed electrostatic excitation $D_n = 4.0$. The shear moduli ratio is $k = 10$, and the dielectric constants ratio is $t = 10$

the critical stretch ratio increases. However, once again at large levels of electric excitations, the trend is reversed (see the curve corresponding to $\bar{\mathbf{D}}_n = 4.0$). In this case, as the lamination angle is decreased from $\Theta = \pi/2$, instabilities may occur at lower stretch ratios.

The influence of the volume fraction of the phases on the stability of the composites is depicted in Fig. 4. Bifurcation diagrams for composites with lamination angles $\Theta = 0, \pi/16, \pi/8$, and $3\pi/16$ subjected to electric excitation $D_n = 4.0$ are plotted as functions of the volume fraction of the stiffer phase (the dashed curve and the continuous curves marked by squares, triangles, and circles, respectively).

At both limits of dilute volume fractions of the stiff and the soft phases the materials are stable. We note, however, that the composites with low volume fractions of the stiffer phase are less stable than

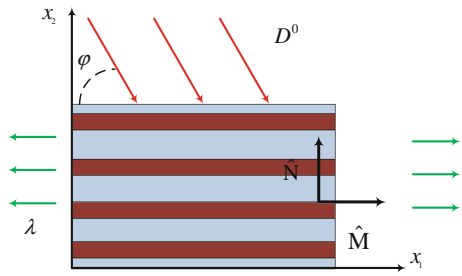

FIG. 5. Electroactive layered composite subjected to electric excitation

those with higher concentration of the stiff phase. This tendency is more pronounced for composites with larger lamination angles, for which at the low concentration end the critical stretch ratio is higher than the one for composites with $\Theta = 0$. Conversely, when the volume fraction of the stiffer phase is higher, the critical stretch ratio is lower than the one determined for $\Theta = 0$ and at high enough volume fractions the material is stable under the applied electrostatic excitation. We emphasize, however, that at higher electrostatic excitations this trend is reversed, and composites with large lamination angle become less stable even with $c^{(f)} > 0.5$. This can be deduced from Fig. 2c that corresponds to materials with $c^{(f)} = 0.8$. Specifically, note the failure surface for $\Theta = 15\pi/128$ (marked with clear triangles) that demonstrates that at $D_n > 10$ the unstable domain of this material is larger than the ones for composites with smaller lamination angles.

Next, we consider the case when the composite is subjected to aligned deformation, *i.e.*, $\Theta = 0$ in Eq. (38) and the angle of applied electric field φ in Eq. (37) varies. A schematic representation of this loading mode is depicted in Fig. 5. In this case, the non-zero components of the electroelastic moduli are

$$\mathscr{E}_{11} = 1/\bar{\varepsilon}, \quad \mathscr{E}_{22} = \mathscr{E}_{33} = 1/\check{\varepsilon}, \tag{42}$$

$$\begin{aligned}
&\frac{1}{2}\mathscr{G}_{111} = \mathscr{G}_{122} = \mathscr{G}_{133} = \mathscr{G}_{212} = \mathscr{G}_{313} = \frac{\bar{D}^0 \lambda \cos\varphi}{\bar{\varepsilon}}, \quad \mathscr{G}_{121} = \mathscr{G}_{211} = \frac{\bar{D}^0 \sin\varphi}{\lambda\bar{\varepsilon}} \\
&\frac{1}{2}\mathscr{G}_{222} = \mathscr{G}_{233} = \mathscr{G}_{323} = \frac{\bar{D}^0 \sin\varphi}{\lambda\check{\varepsilon}},
\end{aligned} \tag{43}$$

$$\begin{aligned}
&\mathscr{A}_{1111} = \mathscr{A}_{3131} = \mathscr{A}_{3232} = \lambda^2\left(\bar{\mu} + \frac{\bar{D}^{0\,2}\cos^2\varphi}{\bar{\varepsilon}}\right), \\
&\mathscr{A}_{1121} = \mathscr{A}_{1211} = \mathscr{A}_{2122} = \mathscr{A}_{2221} = \mathscr{A}_{3132} = \mathscr{A}_{3231} = \frac{\bar{D}^{0\,2}\cos\varphi\sin\varphi}{\bar{\varepsilon}}, \\
&\mathscr{A}_{1313} = \mathscr{A}_{2323} = \mathscr{A}_{3333} = \bar{\mu}, \quad \mathscr{A}_{1212} = \left(\check{\mu} + \frac{\bar{D}^{0\,2}\sin^2\varphi}{\bar{\varepsilon}}\right)\lambda^{-2}, \\
&\mathscr{A}_{1221} = \mathscr{A}_{2112} = \frac{\bar{D}^{0\,2}}{2\lambda^2}\frac{\check{\varepsilon}-\bar{\varepsilon}}{\check{\varepsilon}\bar{\varepsilon}}(1-\cos 2\varphi) + \frac{\check{\mu}-\bar{\mu}}{\lambda^2} \\
&\mathscr{A}_{2121} = \mathscr{A}_{1111} + \mathscr{A}_{1221}, \quad \mathscr{A}_{2222} = \mathscr{A}_{3232} = \left(\bar{\mu} + \frac{\bar{D}^{0\,2}\sin^2\varphi}{\check{\varepsilon}}\right)\lambda^{-2}.
\end{aligned} \tag{44}$$

Obviously, for the cases when $\varphi = n\pi$ and $\pi/2 + n\pi$, where $n = 0, 1, 2, \ldots$, the condition for ellipticity loss (19) reduces to the bi-cubic polynomial Eq. (39). In the case when $\varphi = n\pi$, the critical stretch ratio can be explicitly determined.

$$\lambda_c = \left(1 - \frac{\check{\mu}}{\bar{\mu}}\right)^{1/4}\left(1 + \frac{D^2}{\bar{\mu}\bar{\varepsilon}}\left(1 - \frac{\check{\varepsilon}}{\bar{\varepsilon}}\right)\right)^{-1/4}. \tag{45}$$

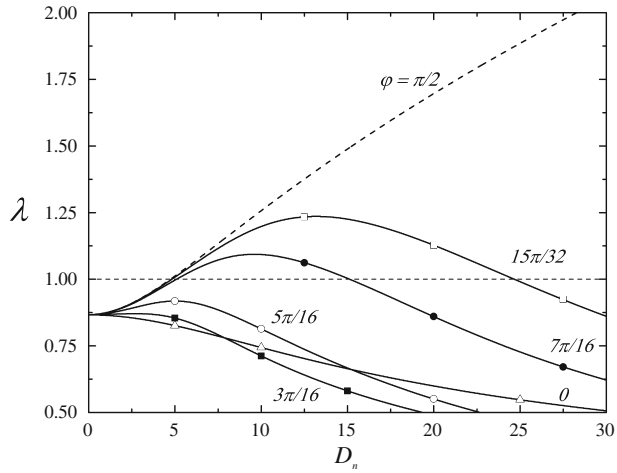

FIG. 6. Bifurcation diagrams of layered materials subjected to aligned stretch and electrostatic excitation at different angles as functions of the critical stretch ratio and electric displacement. The volume fraction of the stiff phase is $c^{(f)} = 0.8$ and the contrasts between the elastic and dielectric moduli are $k = t = 10$

Naturally, this expression is the reciprocal of the one given in Eq. (41).

Bifurcation diagrams as functions of λ_c and D_n are presented in Fig. 6 for composites with $c^{(f)} = 0.8$, and contrast between the shear moduli $k = 10$ and dielectric constants $t = 10$. The diagrams are shown for different angles $\varphi = 0, 3\pi/16, 5\pi/16, 7\pi/16, 15\pi/32$, and $\pi/2$. These correspond to the continuous curves marked by triangles, solid squares, circles, solid circles, squares, and the dashed curve, respectively. The regions beneath the curves correspond to the unstable domains.

The influence of the angle of the applied electric displacement shows that the most sensitive structure is the one with $\varphi = \pi/2$, as its bifurcation curve lies above the ones for $\varphi < \pi/2$. It is easy to see from Fig. 6 that for some values of φ the composite becomes stable even at large intensities of electric excitation. For example, a composite subjected to the electric excitations at $\varphi = 3\pi/16$ is stable even when subjected to large compressive stretch ratios along the layers.

References

1. Agoras, M., Lopez-Pamies, O., Castañeda, P.P.: Onset of macroscopic instabilities in fiber-reinforced elastomers at finite strain. J. Mech. Phys. Solids **57**, 1828–1850 (2009)
2. Bar-Cohen, Y.: EAP history, current status, and infrastructure. In: Bar-Cohen, Y. (ed.) Electroactive Polymer (EAP) Actuators as Artificial Muscles, chapter 1, pp. 3–44. SPIE Press, Bellingham, WA (2001)
3. Bertoldi, K., Boyce, M.C.: Wave propagation and instabilities in monolithic and periodically structured elastomeric materials undergoing large deformations. Phys. Rev. B **78**, 184107 (2008)
4. Bertoldi, K., Gei, M.: Instabilities in multilayered soft dielectrics. J. Mech. Phys. Solids **59**, 18–42 (2011)
5. Bhattacharya, K., Li, J.Y., Xiao, Y.: Electromechanical models for optimal design and effective behavior of electroactive polymers. In: Bar-Cohen, Y. (ed.) Electroactive Polymer (EAP) Actuators as Artificial Muscles, chapter 12, pp. 309–330. SPIE press, Bellingham (2001)
6. Bustamante, R.: Transversely isotropic non-linear electro-active elastomers. Acta Mech. **206**, 237–259 (2009)
7. deBotton, G.: Transversely isotropic sequentially laminated composites in finite elasticity. J. Mech. Phys. Solids **53**, 1334–1361 (2005)
8. deBotton, G., Tevet-Deree, L.: Electroactive polymer composites—analysis and simulation. In: Armstrong W.D. (eds.) Smart Structures and Materials 2006: Active Materials: Behavior and Mechanics, vol. 6170 of Proceedings of SPIE, pp. 2401–2410, San Diego, CA (2006)
9. deBotton, G., Tevet-Deree, L., Socolsky, E.A.: Electroactive heterogeneous polymers: analysis and applications to laminated composites. Mech. Adv. Mater. Struct. **14**, 13–22 (2007)
10. Dorfmann, A., Ogden, R.W.: Nonlinear electroelasticity. Acta Mech. **174**, 167–183 (2005)

11. Dorfmann, A., Ogden, R.W.: Nonlinear electroelastostatics: incremental equations and stability. Int. J. Eng. Sci. **48**, 1–14 (2010)
12. Gei, M., Roccabianca, S., Bacca, M.: Controlling band gap in electroactive polymer-based structures. IEEE-ASME Trans. Mechatron. **16**, 102–107 (2011)
13. Geymonat, G., Müller, S., Triantafyllidis, N.: Homogenization of nonlinearly elastic materials, microscopic bifurcation and macroscopic loss of rank-one convexity. Arch. Ration. Mech. Anal. **122**, 231–290 (1993)
14. Huang, C., Zhang, Q.M., deBotton, G., Bhattacharya, K.: All-organic dielectric-percolative three-component composite materials with high electromechanical response. Appl. Phys. Lett. **84**, 4391–4393 (2004)
15. Kofod, G., Sommer-Larsen, P., Kornbluh, R., Pelrine, R.: Actuation response of polyacrylate dielectric elastomers. J. Intell. Mater. Syst. Struct. **14**, 787–793 (2003)
16. McMeeking, R.M., Landis, C.M.: Electrostatic forces and stored energy for deformable dielectric materials. J. Appl. Mech. Trans. ASME **72**, 581–590 (2005)
17. Mockensturm, E.M., Goulbourne, N.: Dynamic response of dielectric elastomers. Int. J. Nonlinear Mech. **41**, 388–395 (2006)
18. Nestorovic, M.D., Triantafyllidis, N.: Onset of failure in finitely strained layered composites subjected to combined normal and shear loading. J. Mech. Phys. Solids **52**, 941–974 (2004)
19. O'Halloran, A., O'Malley, F., McHugh, P.: A review on dielectric elastomer actuators, technology, applications, and challenges. J. Appl. Phys. **104**, 071101 (2008)
20. Pelrine, R., Kornbluh, R., Joseph, J., Heydt, R., Pei, Q.-B., A., C.: High-field deformation of elastomeric dielectrics for actuators. Mater. Sci. Eng. **11**, 89–100 (2000)
21. Plante, J.-S., Dubowsky, S.: Large-scale failure modes of dielectric elastomer actuators. Int. J. Solids Struct. **43**, 7727–7751 (2006)
22. Rudykh, S., deBotton, G.: Instabilities of hyperelastic fiber composites: micromechanical versus numerical analyses. J. Elast. doi:10.1007/s10659-011-9313-x (2011)
23. Rudykh, S., Bhattacharya, K., deBotton, G.: Snap-through actuation of thick-wall electroactive balloons. To appear in Int. J. Nonlinear Mech. doi:10.1016/j.ijnonlinmec.2011.05.006 (2011)
24. Rudykh, S., Lewinstein, A., Uner, G., deBotton, G.: Giant enhancement of the electromechanical coupling in soft heterogeneous dielectrics. Submitted for publication. http://arxiv.org/abs/1105.4217v1 (2011)
25. Shmuel, G., deBotton, G.: Out-of-plane shear of fiber composites at moderate stretch levels. J. Eng. Math. **68**, 85–97 (2010)
26. Tevet-Deree, L.: Electroactive Polymer Composites—Analysis and Simulation. PhD thesis, Ben-Gurion University (2008)
27. Tian, L., Tevet-Deree, L., deBotton, G., Bhattacharya, K.: Dielectric elastomer composites. Submitted for publication (2010)
28. Toupin, R.A.: The elastic dielectric. Arch. Ration. Mech. Anal. **5**, 849–915 (1956)
29. Triantafyllidis, N., Maker, B.N.: On the comparison between microscopic and macroscopic instability mechanisms in a class of fiber-reinforced composites. J. Appl. Mech. Trans. ASME **52**, 794–800 (1985)
30. Triantafyllidis, N., Nestorovic, M.D., Schraad, M.W.: Failure surfaces for finitely strained two-phase periodic solids under general in-plane loading. J. Appl. Mech. Trans. ASME **73**(3), 505–515 (2006)
31. Vu, D.K., Steinmann, P.: Nonlinear electro- and magneto-elastostatics: material and spatial settings. Int. J. Solids Struct. **44**(24), 7891–7905 (2007)
32. Zhang, S., Huang, C., Klein, R.J., Xia, F., Zhang, Q.M., Cheng, Z.-Y.: High performance electroactive polymers and nano-composites for artificial muscles. J. Intell. Mater. Syst. Struct. **18**, 133–145 (2007)

Stephan Rudykh and Gal deBotton
The Pearlstone Center for Aeronautical Studies
Department of Mechanical Engineering
Ben-Gurion University
84105, Beer-Sheva
Israel
e-mail: debotton@bgu.ac.il

Gal deBotton
Department of Biomedical Engineering
Ben-Gurion University
84105, Beer-Sheva
Israel

(Received: March 26, 2011)